Int. J. Electrochem. Sci., 12 **(2017)** 6352 – 6364, doi: 10.20964/2017.07.74

International Journal of
ELECTROCHEMICAL
SCIENCE
www.electrochemsci.org

Short Communication

Influence of Reaction Temperature on the Controlled Growth of Mg-Al LDH Film

Liang Wu[*], *Zhicheng Zheng, Fusheng Pan*[**], *Aitao Tang, Gen Zhang, Lei Liu*

School of Materials Science and Engineering, Chongqing University, Chongqing 400044, China.
[*]E-mail address: wuliang@cqu.edu.cn.
[**]E-mail address: fspan@cqu.edu.cn.

Received: 23 February 2017 / *Accepted:* 24 April 2017 / *Published:* 12 June 2017

The Mg-Al layered double hydroxides (Mg-Al LDH) film was fabricated on anodized magnesium alloy AZ31 at different reaction temperature by in-situ hydrothermal treatment method. The reaction solution contained only one kind of trivalent cation Al^{3+}, and the divalent cation Mg^{2+} is provided by the anodic oxide films. The structure, composition and morphology of the Mg-Al LDH films were investigated via XRD, FI-IR and SEM, respectively. The corrosion resistance of films was studied using potentiodynamic polarization and electrochemical impedance spectroscopy. The SEM images show that the compactness of LDHs increases with the increase of the reaction temperature. The results of XRD and FT-IR indicate that the crystallinity of films was improved with the increase of reaction temperature. The results of potentiodynamic polarization and electrochemical impedance spectrum show that the corrosion resistance was improved with the increase of reaction temperature. The influence mechanism of reaction temperature on the controlled growth of Mg-Al LDH films was investigated subsequently.

Keywords: magnesium alloy; reaction temperature; layered double hydroxides; corrosion resistance; anodic oxide film

1. INTRODUCTION

Magnesium and its alloys have lower density, which is two-thirds of the density of aluminum and a quarter of the density of iron. Magnesium alloys possess a series of properties such as high specific strength and stiffness, damping capacity, electrical and thermal conductivity, damping ability, electromagnetic shielding and easy to recycle, etc. Due to the unique properties, magnesium and magnesium alloys go by the name of “Green engineering materials in twenty-first Century” [1,2]. In recent years, as the application requirement of the industries of automotive automation, aerospace, electric tools, recreation facilities, mobile phone, computer, etc, magnesium and its alloys have

attracted considerable attention [3]. However, magnesium alloys have high chemical and electrochemical activity. Poor corrosion resistance impedes seriously its wide application in the actual industrial production [4]. Therefore, improving the corrosion resistance of magnesium alloys has become one of the key research of magnesium alloys in the world [5,6]. At present, the most widespread method to improve corrosion protection of magnesium alloy surface is anodizing technology [7,8]. However, this technology has the problems of poor stability, poor adhesion and insufficient thickness [9,10]. The protection of film for substrate would be influenced greatly due to those problems. It is necessary for improving corrosion resistance of anodic oxide film by sealling holes.

The fabrication of the LDHs on the anodic oxide film could solve the problem effectively. The layered double hydroxides (LDHs) film is a typical two dimensional layered nano material [1,11]. LDHs can be expressed by the general formula $[M^{2+}_{1-x}, M^{3+}_{x}(OH)_2]^{x+}$ $(A)^{n-}_{x/2}\cdot mH_2O$, where the cations M^{2+} and M^{3+} occupy the octahedral holes in the position of octahedral brucite and the anion $A^{n-}$is located in the hydrated interlayer galleries [12,13]. Recently, extensive studies have focused on the potential applications of LDHs as films to protect metals such as magnesium alloys [14], aluminum alloys [15] and steel [16,17]. Layered double hydroxides (LDHs) are a kind of anionic layered structure material, and in recent years, it has attracted much attention as a new type of inorganic nanocontainer with special structure characteristics, especially the ion exchange capacity [18]. When contacting with erosive ions such as Cl^- in environmental media, LDHs would release inter-layer anion and adsorb Cl^- from environment media. Therefore, a new generation of active corrosion inhibition films system is expected to be constructed by assembling different corrosion inhibitor molecules into layers, and preparing a corrosion inhibitor loaded LDH intelligent "nanocontainer". So far, three main methods have been developed to prepare LDH films: (i) the in-situ growth method, (ii) the co-precipitation method [19], and (iii) the two-step method [20]. In this study, the LDH films were fabricated by the in-situ growth method on the anodized magnesium alloy AZ31. On the one hand, the method could not only add a protective film, but also the loose porous holes could be sealed effectively by the LDHs nanosheets. On the other hand, one of the most important reason for LDH films to protect the substrate from corrosion is that it can be used as a nanocontainer which load inhibitor ion [21]. Inorganic nanocontainer, which is widely used in study on the load and controlled release of corrosion inhibitor [22-24], has the advantages of small size, high load, easy to modify and so on. Generally, both of the M^{3+} and M^{2+} are needed in the preparation of LDH which grow on the surface of metal substrate. However, in this study, we prepared an anodic oxide film on the metal substrate firstly, and then the LDHs film was fabricated on the anodic oxide film. Furthermore, only the Al^{3+} is added into the reaction solution and the Mg^{2+} could be provided by the anodic oxide film. Compared to the traditional methods, this method is more facile.

The size and the distribution of the LDHs crystal could be controlled by the reaction conditions for preparing LDH films [25,26]. According to the theories of crystallography, the nucleation rate and growth rate of crystal could be controlled by adjusting the reaction temperature. Therefore, the sizes and the distributions of the LDHs crystal could be controlled effectively within a certain range of reaction temperature [27]. Recently, Naosumi Kamiyama and his colleagues [28] studied the effect of treatment time in the Mg-Al LDH composite film formed on Mg alloy AZ31 by

steam coating on the corrosion resistance. Their results show that the thickness of the Mg-Al LDH films increase with the reaction time from 1h to 9h. And at the earlier time, J. Tedim and his colleagues [29] had discussed the influence of preparation conditions of LDH conversion films on corrosion protection. They found that the increase of Zn^{2+} concentration used in the growth of LDH film could lead to thicker and more compact films and the better anticorrosion performance was obtained because of LDH thin films. By the way, since both of them fabricated the LDH film on the metal substrate, the corrosive ions could still contact with the substrate with a little of damage of LDH film. We prepared LDH film on the surface of anodic oxide film, and this method could achieve the perfect combination of the advantages of LDH film and anodic oxide film. Further, in the studies of Naosumi Kamiyama and J. Tedim, the effects of treatment time and concentration of reactants on the growth of LDH film have been researched, but it is obvious that the reaction temperature has a huge impact on the growth of the LDH film. However, the effect of temperature on the growth of LDH film has not been thoroughly studied and this work is urgent to be done.

In this study, Mg-Al layered double hydroxides (Mg-Al-LDHs) film was prepared successfully via the in-situ growth method. The effect of reaction temperature on the growth of Al-Mg-LDH films was studied. The controllable growth of Mg-Al-LDH films was achieved by adjusting the reaction temperature. Meanwhile, LDH material has many structural advantages such as the dispersion of metal elements in the metal layer, the control of the metal elements and the interlayer anion. These structural advantages contribute to preparing a series of LDH materials and corrosion inhibitor loaded LDH functional coatings. And the research and application of Mg-Al-LDH in the field of protective film are realized consequently. The regulation and control of the active protective function of the film is realized by exploring the structural growth conditions of Mg-Al-LDH. We successfully confirmed the influence of treatment temperature for preparing LDH films on corrosion resistance.

2. EXPERIMENTAL

2.1. Materials

The experimental magnesium alloy AZ31 (the nominal compositions in wt.%: Al 2.5-3.5, Zn 0.6-1.3, Mn 0.2-1, Ca 0.04, Si 0.1, Cu 0.05, and balanced Mg) with the sizes of 10 mm × 10 mm × 2 mm and 20 mm × 20 mm × 2 mm were used as the substrate. The surface of each specimen was grinded to 2000# by silicon carbide abrasive paper.

2.2. Procedures

Preparation of anodic oxide film: The DC regulated power was used in anodizing process. The anodic oxide film of magnesium alloy AZ31 sample was prepared in mixture solutions of 7.14 g/L NaOH and 4 g/L $NaAlO_2$ for 30 min with applied voltage of 20V. Then, ultrasonically cleaned in ethyl alcohol for 5 min and dried under a steam of air.

Preparation of Mg-Al-LDH films: 0.05 mol/L $Al(NO_3)_3 \cdot 6H_2O$ and 0.3 mol/L NH_4NO_3 were dissolved into 100 mL deionized water, and dilute ammonia solution was used to adjust the pH of solution. Then the mixed solution was poured into Teflon-lined autoclave in which the anodic oxide magnesium alloy was immersed. And the Teflon-lined autoclave was then hermetically heated at 105℃, 115℃, 125℃, 135℃ and 145℃for 12 h, respectively. Take the samples out after cooling them to room temperature. The surfaces of samples were washed with pure water and ethanol in turn, and then the samples were rinsed by ultrasonic cleaning machine. The Al-Mg/NO_3^- LDH films were fabricated at different crystallization temperatures via above steps.

2.3. Characterization

Surface morphology of films was observed by JSM-7800F field emission scanning electron microscopy (FE-SEM, Nova 400 FEI USA). All the samples were treated with gold spray. The crystal structures of the LDH films were examined using an X-ray diffractometer (XRD, D/Max 2500X Rigaku Japan) at a glancing angle of 1.5o using Cu target (λ=0.154 nm) with 40 kV and 150 mA radiation. The qualitative analysis of sample composition was conducted via American Nicolet IS5 model Fourier infrared spectrometer (FT-IR, Nicolet IS5 Thermo Scientific USA) with variable angle ATR in the range of 4000-400 cm^{-1}.

Electrochemical tests were carried out on the SI 1287 originated from American Princeton company and Shanghai Chen Hua CHI660 electrochemical systems. A three electrode system was used in this test, which reference electrode as saturated calomel electrode (SCE), auxiliary electrode as high purity platinum sheet and test sample as the working electrode (1 cm^2). The solution of test is 3.5 wt.% NaCl solution. After the open circuit potential (OCP) was stabilized, the electrochemical impedance spectroscopy (EIS) was performed. The polarization curves were recorded with a sweep rate of 2 mV/s. EIS measurements were acquired from 100 kHz down to 10 mHz using a 5 mV amplitude perturbation with three parallel samples in each group. the obtained EIS data was fitted by the equivalent circuit via Z-View software to obtain the required parameters.

3. RESULTS AND DISCUSSION

3.1. XRD analysis

Fig.1 shows XRD spectra of the Mg-Al LDH samples fabricated at different reaction temperatures. And all of the XRD spectra have clear diffraction peaks. The sharp characteristic diffraction peaks such as LDH (003) and LDH (006) indicate that samples have a complete layer structure and good crystal structure [30]. Moreover, with the increase of temperature, the characteristic diffraction peak of crystal surface becomes sharp. This result shows that the crystallinity of LDH and the completeness of crystal structure increase with the increasing temperature. (003) and (006) characteristic diffraction peaks are located at about 10 and 20 degrees, respectively. These results are consistent with the results of NO_3^- intercalated LDH in the literature [31]. So the interlayer anion in obtained LDH film can be determined as NO_3^-.

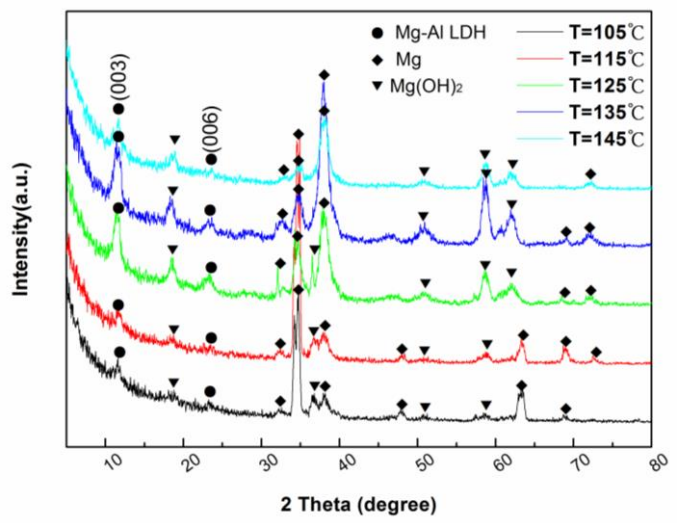

Figure 1. The XRD spectra of Mg-Al LDH film samples formed on anodized magnesium alloy AZ31 obtained at different reaction temperatures (T=105℃, 115℃, 125℃, 135℃,145℃). Peaks marked with ● are due to the Mg-Al LDH film, ◆are due to Mg phase and ▼ are due to the $Mg(OH)_2$

3.2. FT-IR analysis

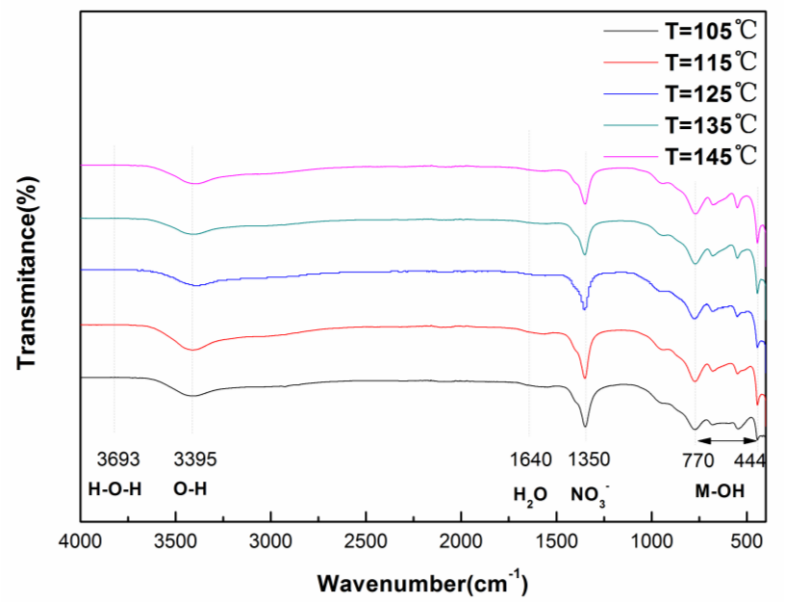

Figure 2. ATR-FTIR spectra of Mg-Al LDH film samples obtained at different reaction temperatures (T=105℃, 115℃, 125℃, 135℃, 145℃)

Fig.2 is the FT-IR spectra of LDH films formed at different crystallization temperatures. This figure shows the typical characteristic absorption peak of LDHs. The absorption band at 3693 cm^{-1} is caused by the H-O-H stretching vibration [1]. The wide spectrum absorption band at 3395 cm^{-1} and the absorption band at around 1641 cm^{-1} are caused by the hydroxyl group stretching absorption and the

flexural oscillation peaks of the interlayer water molecule O-H [32]. The absorption band at 3395 cm^{-1} is caused by hydroxyl metal functional groups and hydrogen bonding between water molecules. Additionally, the absorption band at 1350 cm^{-1} corresponds to the asymmetric stretching band of intercalated NO_3^- [33]. The spectral peaks of 444~770cm^{-1} correspond to the lattice vibration absorption peaks of LDHs metal oxygen bonds (M-O, M-O-M and O-M-O). It is obvious that there is a certain amount of intercalated NO_3^- anion in all of samples. This result confirms that LDH films could be fabricated at a series of experimental temperature conditions.

3.3. SEM analysis

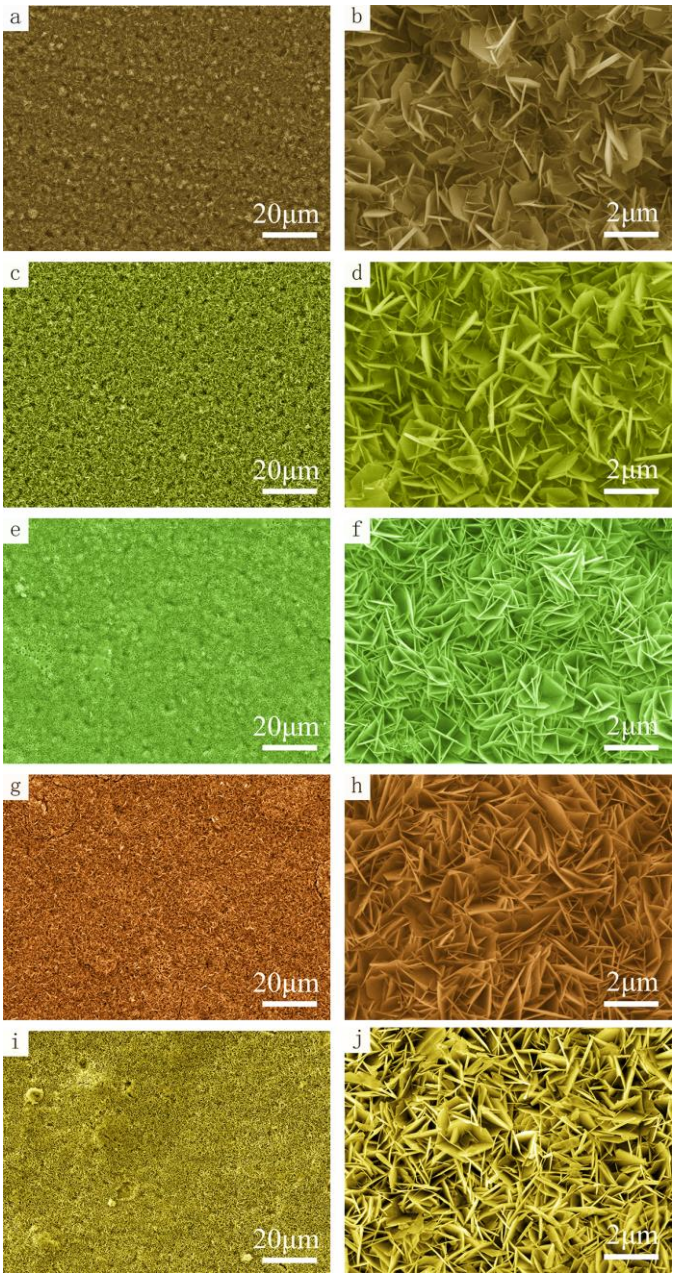

Figure 3. SEM images of LDH films obtained at different crystallization temperatures with low and high power microscope: (a) and (b) T=105℃, (c) and (d) T=115℃, (e) and (f) T=125℃, (g) and (h) T=135℃, (i) and (j) T=145℃

Fig.3 indicates that the loose pores of anodic oxide films have been closed mostly by LDH films. The surface of films is covered by fine and compact lamellar structure. The LDH crystallites is obvious curl and blade-like structure which are formed by the combination of metal hydroxide and inlayer ion [34]. With the reaction temperature gradually increasing, the holes of the anodic oxide films become smaller. When T=105℃ and 115℃, the holes of the films of samples are larger and obvious; while T=125℃, there are just some bumps on the surface; when T=135℃ and 145℃, the bumps can't be observed obviously from the surface of samples. The result reveals that the crystallinity of LDHs increases with the increase of the reaction temperature, and it is consistent with the result of XRD shown in Fig.1 and the conclusion of the spectral peak at 444~770cm^{-1} is shown in Fig.2.

3.4. Tafel polarization curve

The corrosion resistance of LDH film prepared at different temperatures was investigated by electrochemical test. The Tafel polarization curves of the initial state of the Mg-Al LDH film samples obtained at different reaction temperatures are shown in Fig.4, and the corrosion potential E_{corr}, corrosion current density I_{corr}, cathodic Tafel slope b_c and anode Tafel slope b_A of different samples are list in Table 1.

Table 1. The data of Tafel polarization curve results of different samples. E_{corr}: the corrosion potential, I_{corr}: corrosion current density, b_c: cathodic Tafel slope and b_A: anode Tafel slope

Temperature	Test solution	E_{corr} (V/SCE)	I_{corr} (μA/cm2)	b_c(V/decade)	b_A(V/decade)
T=105℃	3.5wt.%NaCl	-1.278	19.36	0.104	0.490
T=115℃	3.5wt.%NaCl	-0.807	1.459	0.171	0.222
T=125℃	3.5wt.%NaCl	-0.701	2.157	0.187	0.264
T=135℃	3.5wt.%NaCl	-0.588	2.199	0.176	0.224
T=145℃	3.5wt.%NaCl	-0.318	1.036	0.156	0.253

As shown in Table 1, corrosion potentials of the samples coated with LDH film fabricated at 105℃, 115℃, 125℃, 135℃ and 145℃ are -1.278 V vs. SCE, -0.807V vs. SCE, -0.701V vs. SCE, -0.588 V vs. SCE and -0.318V vs. SCE, respectively. The corrosion potential increases with the increasing temperature. This result confirmed that the corrosion resistance of the LDH films is increased and the effective barrier between the substrate and the corrosion medium is realized. Moreover, the corrosion potential and corrosion current density of LDH film obtained at 145℃ are respectively maximum and minimum, and this result confirms that the corrosion resistance of LDH film obtained at 145℃is the best than the other samples. It is consistent with the results of Fig.1, Fig.2

and Fig.3. The data of cathodic Tafel slope b_c and anode Tafel slope b_A are list in the Table 1, all of the values of the anode Tafel slopes b_A are higher than the corresponding cathodic Tafel slopes b_c, therefore, the corrosion resistance of film depends on the rate the anodic dissolution mostly. Relatively, the data floating of b_A is larger than the value of b_c, and the result indicates temperature could improve the corrosion resistance of the film by controlling the anodic dissolution. As for the reasonable explanation of the above results, on the one hand, the ion exchange ability of LDH film greatly improve the corrosion resistance of films [35]. On the other hand, as a result of the LDH film increases the thickness of the protective layer, the difficulty of the contact between the corrosive ion and the substrate is improved.

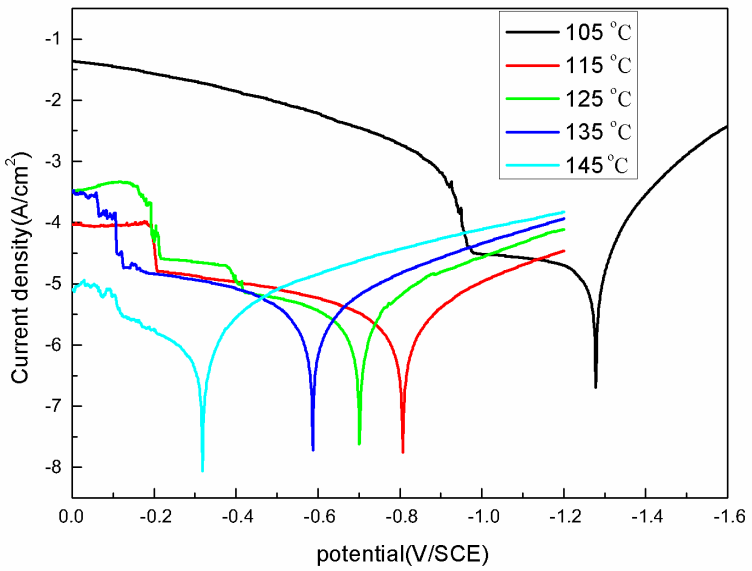

Figure 4. The Tafel polarization curves of the initial state of the Mg-Al LDH film samples obtained at different reaction temperatures (T=105℃, 115℃, 125℃, 135℃,145℃)

3.5. EIS analysis

In order to further investigate the corrosion resistance of LDH films formed at different temperature. The EIS test for the different samples has been done and the results are shown in Fig.5. As observed in Frequence-Phase Bode figure, the data of Al-Mg LDH film, which is grown on the anodic oxide film, has two time constants. In general, the outer layer of the film is corresponding to the high frequency region [20]. As shown in the Fig.3, we could find that the LDH layer is relatively loose and thick, and it is obviously different from the dense anodic oxide layer at the bottom. The difference between the two is corresponding to the difference between the impedance of high frequency and intermediate frequency. At low frequency, the higher the |Z| value is, the better corrosion resistance of the material is [1]. It's obvious that the |Z| value of the LDH film obtained at 145℃ is higher than others. In addition, the |Z| values of the LDH film obtained at different temperature follow a general tendency: the higher the reaction temperature is, the higher the corresponding |Z| value is. This result is consistent with the Tafel polarization curve result.

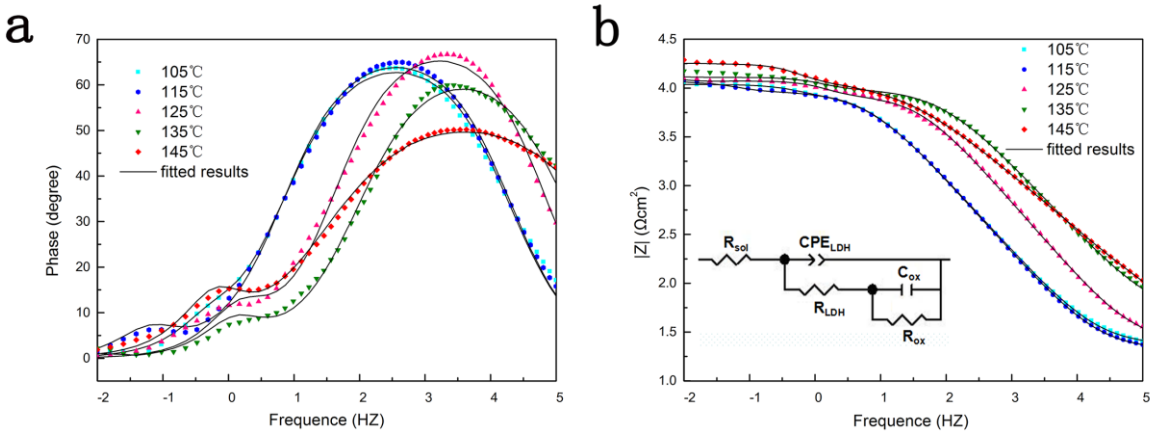

Figure 5. Bode Figure and the fit figure (a, b) of different samples obtained at different temperature (T=105℃, 115℃, 125℃, 135℃,145℃) by being soaked in 3.5wt.% NaCl solution and the equivalent circuit for the samples coated with LDH film

It is helpful for us to analyze the role of each layer in the corrosion resistance by using the Zview circuit simulation software to simulate the equivalent circuit diagram, and then the protective mechanism of the film would be proposed. Generally, the component of equivalent circuit is not only related to the time constant of Bode diagram, but also combined with the situation of the data display of electrochemical impedance spectroscopy [36]. Then we could get more accurate fitting data.

As shown in the Fig.5, after a comprehensive analysis, the equivalent circuit is set up. The equivalent circuit includes the following components: R_{sol} in the equivalent circuit diagram is the solution resistance; CPE_{LDH} and R_{LDH} are respectively the capacitance and resistance of LDH films; C_{ox} and R_{ox} are respectively the capacitance and resistance of anodic oxide layer. In order to reflect the heterogeneity of components, the constant phase angle element (CPE) is introduced, which is used to replace the pure capacitance C, the impedance of the constant-phase element is defined in Eq. (1) [37],

$$Z_{CPE} = [C(j\omega)^{\alpha}]^{-1} \quad (1)$$

Where, the constant C is the magnitude of CPE, α is the empirical exponent of the CPE, $0<\alpha<1$. If $\alpha=1$, C is the pure capacitance; if $\alpha=0$, C is the pure resistance.

The electrochemical impedances for LDH films are given by Eq. (2),

$$Z = R_{sol} + \frac{1}{\frac{1}{Z_{CPE}} + \frac{1}{\frac{1}{R_{LDH}} + \frac{1}{\frac{1}{R_{ox}} + \frac{1}{Z_C}}}} = R_{sol} + \frac{1}{(j\omega)^{\alpha} C_{LDH} + \frac{1}{R_{LDH} + \frac{1}{\frac{1}{R_{ox}} + j\omega C_{ox}}}} \quad (2)$$

According to Eq. (2), the impedance of LDH film increases with the increase of the polarization resistance (R_{LDH}, R_{ox}) and the decrease of the capacitance (C_{LDH}, C_{ox}). It can be observed from the fitting data of samples as list in Table 2. The R_{LDH} value of the LDH layer is high and the C_{LDH} value is extremely low indicate that the LDH film have an effective corrosion prevention for the substrate. The arrangement of the LDH nanosheets of bottom layers is very tight, and the corresponding R_{LDH} value is also high. The R_{LDH} is the resistance of the LDH films, and the value of the R_{LDH} is increasing tremendously with higher temperature. This result could verify that the higher the temperature is, the better the corrosion resistance of LDH films is. When the temperature is 145℃, the value of R_{LDH} is highest and the C_{LDH} of the sample prepared at 145℃ is relatively low. This result indicates that LDHs film prepared at 145℃ covers anodic oxide films effectively and has the best resistance to corrosion.

Table 2. Impedance parameters of Mg-Al LDH film obtained at different reaction temperature (T=105 ℃, 115℃, 125℃, 135℃, 145℃) via the data of EIS fitted with the equivalent circuit

Mg-Al LDH samples	R_{sol}/Ωcm^2	CPE_{LDH}		R_{LDH}/Ωcm^2	C_{ox}/μFcm^{-2}	R_{ox}/μFcm^{-2}
		C_{LDH}/μFcm^{-2}	α_{LDH}			
T=105℃	22.83	6.4507×10^{-6}	0.7535	9363	2.0009×10^{-4}	1581
T=115℃	20.73	6.1622×10^{-6}	0.7634	9367	1.3291×10^{-3}	2106
T=125℃	24.45	1.4926×10^{-6}	0.7870	8712	4.0168×10^{-5}	3130
T=135℃	44.01	9.6734×10^{-7}	0.7307	10047	5.1340×10^{-5}	2803
T=145℃	28.11	3.8708×10^{-6}	0.5992	12332	5.2469×10^{-5}	5720

On the other hand, the R_{sol} value of the LDH layer grown on the anodic oxide films is high. It shows that LDH film is not only limited to grow at the surface of the anodic oxide film, but also in the pores of the porous anodic oxide films, thereby the structure of the porous anodic oxide films is affected. With the growth of LDH film, the pores in the anodic oxide films will gradually be closed, and the growth of LDH crystals is in a state of equilibrium. Other scholars have found similar phenomena [38], too.

3.6. The influence mechanism of reaction temperature.

A schematic illustration of the influence mechanism of reaction temperature on the controlled growth of the Mg-Al LDH film is shown in Fig.6. According to the results of the XRD and the images of SEM, the crystallinity of the LDH films has an obvious rise with the increasing reaction temperature. According to the research of J. Chen and his colleagues [39], after immersed in the reaction solution for some time, the anodic oxide film will be decomposed and release the Mg^{2+}. The dissociative Mg^{2+} provide sources for the formation of the original LDH granules by diffusing into the $Al(OH)_3$. The original LDH granules could grow bigger and form the LDH nanosheets finally. Eliseev [40] proposed the similar mechanism of the formation of LDH granules.

The anodic oxide film is dissolved and the Mg^{2+} cations are produced while the anodic oxide film of the magnesium alloy AZ31 obtained in alkaline solution consists of magnesium hydroxide and magnesium oxide [41]. Whatever, since the decomposition reaction of the oxides is an endothermic process, the increasing reaction temperature could promote the decomposition reaction. Consequently, the distribution density of the decomposition points on the anodic oxide film would increase. In other words, the distribution density of the LDH crystal nucleus will increase with the increasing reaction temperature. The change of morphologies of LDH films is shown in the image of SEM. After the LDH crystal nucleus grows up into the LDH sheets, as shown in the Fig.6, the interspace between the LDH sheets is inversely proportional to the distribution density of the LDH crystal nucleus. Firstly, since the interspace between the LDH sheets is too large, the aggressive ions could reach the anodic oxide film easily. However, the anodic oxide film has cracks and holes so that the aggressive ions have a larger possibility to penetrate through the anodic oxide film and contact with the metal substrate. Secondly, the quantity of the nanocontainer would have a decline when the interspace between the LDH sheets becomes larger. The ion exchange capacity of LDH film is weakened. In short, the increasing reaction temperature could improve the corrosion resistance of the LDH film. This result is agreed on the results as shown in Fig.5 and Table 2.

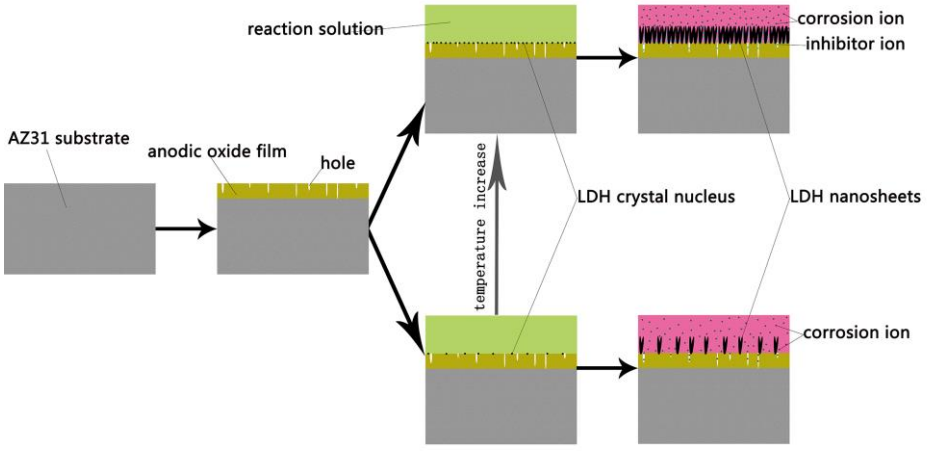

Figure 6. Schematic illustration of the influence mechanism of reaction temperature on the controlled growth of the Mg-Al LDH film

4. CONCLUSIONS

In this study, the impact factors of the orientation structure of LDH films are studied systematically. The main conclusions are obtained through experiments and characterization analysis as following:

(1) The results of SEM and XRD indicate that the morphology and orientation structure of LDH films grown on the magnesium alloy at different reaction temperatures have great differences. The result indicates that appropriate high temperature is favorable for the crystallization of LDH grains and confirms that the crystal orientation of LDH film can be influenced by crystallization temperature.

(2) The effect of crystallization temperature on the orientation structure and compactness of LDH film was studied systematically. The size and density of the grain of LDH film could be effectively controlled via changing the reaction temperature, and the controllable preparation of LDH based films was realized.

(3) The compactness of the Mg-Al-NO_3^- LDH film fabricated on the magnesium alloy AZ31 by in-situ growth at different reaction temperature is admirable. Moreover, the films could provide effective corrosion protection for magnesium alloy substrate. With the increase of reaction temperature, the resistance of the film gradually increases, and the corrosion resistance is obviously improved.

ACKNOWLEDGEMENT
This work was supported by the Student's Platform for Innovation and Entrepreneurship Training Program under Grant <No 201610611043>; the Chongqing Research Program of Basic Research and Frontier Technology under Grant <No cstc2016jcyjA0388>, and the Fundamental Research Funds for the Central Universities under Grant <No 106112017CDJXY130002>.

References

1. F. Zhang, Z. G. Liu, R. C. Zeng, S. Q. Li, H. Z. Cui, L. Song and E. H. Han, *Surf. Coat. Technol.*, 258 (2014) 1152.
2. J. K. Lin, J. Y. Uan, C. P. Wu and H. H. Huang, *J. Mater. Chem.*, 21 (2011) 5011.
3. D. Y. Hwang, Y. M. Kim and D. H. Shin, *Mater. Trans.*, 50 (2009) 671.
4. B. S. Liu, Y. F. Kuang, Y. S. Chai, D. Q. Fang, M. G. Zhang and Y. H. Wei, *J. Magnes. Alloy*, 4 (2016) 220.
5. A. Atrens, G. L. Song, F. Cao, Z. Shi and P. K. Bowen, *J. Magnes. Alloy*, 1 (2013) 177.
6. A. Atrens, M. Liu and N. I. Z. Abidin, *Mater. Sci. Eng., B*, 176 (2011) 1609.
7. I. S. Park, Y. S. Jang, Y. K. Kim, M. H. Lee, J. M. Yoon and T. S. Bae, *Surf. Interface Anal.*, 40 (2008) 1270.
8. W. Xue, Z. Deng, R. Chen and T. Zhang, *Thin solid films*, 372 (2000) 114.
9. C. Blawert, W. Dietzel, E. Ghali and G. Song, *Adv. Eng. Mater.*, 8 (2006) 511.
10. K. Yasui, K. Nishio, H. Nunokawa and H. Masuda, *J. Vac. Sci. Technol., B*, 23 (2005) L9.
11. D. Scarpellini, C. Falconi, P. Gaudio, A. Mattoccia, P. G. Medaglia, A. Orsini, R. Pizzoferrato and M. Richetta, *Microelectron. Eng.*, 126 (2014) 129.
12. Y. Dong, F. Wang and Q. Zhou, *J. Coat. Technol. Res.*, 11 (2014) 793.
13. F. Wu, J. Liang, Z. Peng and B. Liu, *Appl. Surf. Sci.*, 313 (2014) 834.
14. J. K. Lin, K. L. Jeng and J. Y. Uan, *Corros. Sci.*, 53 (2011) 3832.
15. H. Chen, F. Zhang, S. Fu and X. Duan, *Adv. Mater.*, 18 (2006) 3089.
16. T. T. X. Hang, T. A. Truc, N. T. Duong, N. Pébère and M. G. Olivier, *Prog. Org. Coat.*, 74 (2012)

343.
17. M. F. Montemor, D. V. Snihirova, M. G. Taryba, S. V. Lamaka, I. A. Kartsonakis, A. C. Balaskas, G. Kordas, J. Tedim, A. I. Kuznetsova, M. L. Zheludkevich and M. G. S. Ferreira, *Electrochim. Acta*, 60 (2012) 31.
18. S. L. Wang, C. H. Lin, Y. Y. Yan and M. K. Wang, *Appl. Clay. Sci.*, 72 (2013) 191.
19. S. O'Leary, D. O'Hare and G. Seeley, *Chem. Commun.*, 14 (2002) 1506.
20. Y. Zhang, J. Liu, Y. Li, M. Yu, S. Li and B. Xue, *J. Coat. Technol. Res.*, 12 (2015) 595.
21. E. Alibakhshi, E. Ghasemi, M. Mahdavian and B. Ramezanzadeh, *Corros. Sci.*, 115 (2017) 159.
22. I. A. Kartsonakis, E. P. Koumoulos, A. C. Balaskas, G. S. Pappas, C. A. Charitidis and G. C. Kordas, *Corros. Sci.*, 57 (2012) 56.
23. D. G. Shchukin, M. Zheludkevich and H. Möhwald, *J. Mater. Chem.*, 16 (2006) 4561.
24. E. D. Mekeridis, I. A. Kartsonakis and G. C. Kordas, *Prog. Org. Coat.*, 73 (2012) 142.
25. M. Adachi-Pagano, C. Forano and J. P. Besse, *J. Mater. Chem.*, 13 (2003) 1988.
26. K. Okamoto, N. Iyi and T. Sasaki, Appl. *Clay. Sci.*, 37 (2007) 23.
27. Z. L. Hsieh, M. C. Lin and J. Y. Uan, *J. Mater. Chem.*, 21 (2011) 1880.
28. N. Kamiyama, G. Panomsuwan, E. Yamamoto, T. Sudare, N. Saito and T. Ishizaki, *Surf. Coat. Technol.*, 286 (2016) 172.
29. J. Tedim, M. L. Zheludkevich, A. C. Bastos, A. N. Salak, A. D. Lisenkov and M. G. S. Ferreira, *Electrochim. Acta*, 117 (2014) 164.
30. M. Ogawa and H. Kaiho, *Langmuir*, 18 (2002) 4240.
31. J. B. Han, J. Lu, M. Wei, Z. L. Wang and X. Duan, *Chem. Commun.*, 41 (2008) 5188.
32. L. Wang, K. Zhang, H. He, W. Sun, Q. Zong and G. Liu, *Surf. Coat. Technol.*, 235 (2013) 484.
33. H. Chen, F. Zhang, T. Chen, S. Xu, D. G. Evans and X. Duan, *Chem. Eng. Sci.*, 64 (2009) 2617.
34. Z. P. Xu and H. C. Zeng, *Chem. Mater.*, 13 (2001) 4555.
35. M. L. Zheludkevich, S. K. Poznyak, L. M. Rodrigues, D. Raps, T. Hack, L. F. Dick and M. G. S. Ferreira, *Corros. Sci.*, 52 (2010) 602.
36. E. Alibakhshi, E. Ghasemi, M. Mahdavian, B. Ramezanzadeh and S. Farashi, *J. Electrochem. Soc.*, 163 (2016) C495.
37. V. Raman, S. Nagarajan and N. Rajendran, *Electrochem. Commun.*, 8 (2006) 1309.
38. P. Ding, Z. Li, Q. Wang, X. Zhang, S. Tang, N. Song and L. Shi, *Mater. Lett.*, 77 (2012) 1.
39. J. Chen, Y. Song, D. Shan and E. H. Han, *Corros. Sci.*, 63 (2012) 148
40. A. A. Eliseev, A. V. Lukashin, A. A. Vertegel, V. P. Tarasov and Y. D. Tret'Yakov, *Dokl. Chem.*, 387 (2002) 339.
41. Y. Mizutani, S. J. Kim, R. Ichino and M. Okido, *Surf. Coat. Technol.*, 169 (2003) 143.